

Universal Incremental Learning: Mitigating Confusion from Inter- and Intra-task Distribution Randomness

Sheng Luo^{1,2}, Yi Zhou^{1,2*}, Tao Zhou³

¹School of Computer Science and Engineering, Southeast University, China

²Key Laboratory of New Generation Artificial Intelligence Technology and Its Interdisciplinary Applications (Southeast University), Ministry of Education, China

³Nanjing University of Science and Technology, Nanjing, China

Abstract

Incremental learning (IL) aims to overcome catastrophic forgetting of previous tasks while learning new ones. Existing IL methods make strong assumptions that the incoming task type will either only increase new classes or domains (i.e. Class IL, Domain IL), or increase by a static scale in a class- and domain-agnostic manner (i.e. Versatile IL (VIL)), which greatly limit their applicability in the unpredictable and dynamic wild. In this work, we investigate **Universal Incremental Learning (UIL)**, where a model neither knows which new classes or domains will increase along sequential tasks, nor the scale of the increments within each task. This uncertainty prevents the model from confidently learning knowledge from all task distributions and symmetrically focusing on the diverse knowledge within each task distribution. Consequently, UIL presents a more general and realistic IL scenario, making the model face confusion arising from inter-task and intra-task distribution randomness. To **Mitigate both Confusion**, we propose a simple yet effective framework for UIL, named **MiCo**. At the inter-task distribution level, we employ a multi-objective learning scheme to enforce accurate and deterministic predictions, and its effectiveness is further enhanced by a direction recalibration module that reduces conflicting gradients. Moreover, at the intra-task distribution level, we introduce a magnitude recalibration module to alleviate asymmetrical optimization towards imbalanced class distribution. Extensive experiments on three benchmarks demonstrate the effectiveness of our method, outperforming existing state-of-the-art methods in both the UIL scenario and the VIL scenario. Our code will be available at [here](#).

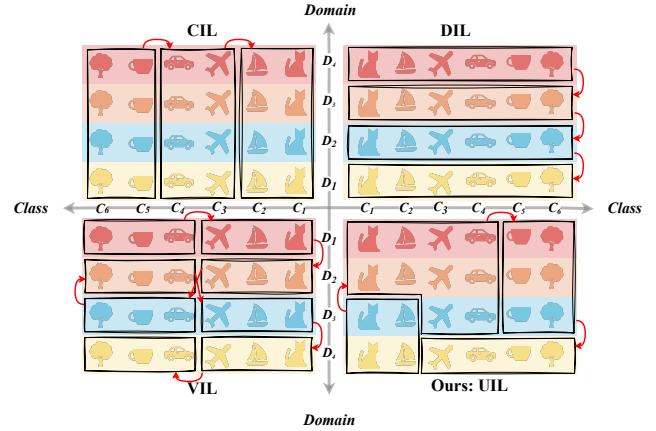


Figure 1. Comparison of existing IL scenarios and our UIL scenario on a 6-class dataset with 4 domains. The horizontal axis denotes class index and the vertical axis denotes domain index. Each incremental task is outlined in black. CIL, DIL, and VIL assume that each incoming task introduces only class increments, domain increments, or both class and domain increments, respectively. In contrast, UIL is a more general IL scenario than existing ones by simultaneously introducing randomness in both the type and scale of increments, as the model neither knows which new classes or domains will increase across all task distributions, nor the number of new classes or domains within each task distribution.

1. Introduction

Incremental learning (IL) [3, 8, 15, 29, 33, 37, 38, 40] aims to continuously learn new knowledge over time. This paradigm is particularly crucial in the dynamic real-world scenario, as it allows a single model to incrementally learn all sequentially arrived tasks, without the need to respectively train task-specific models from scratch.

Based on the type of increments, mainstream IL sce-

*Corresponding author: Yi Zhou (yizhou.szcen@gmail.com)

narios are categorized into class-incremental learning (CIL) [33, 38, 39] and domain-incremental learning (DIL) [6, 37], as illustrated in Fig. 1: 1) CIL assumes that each incremental task only introduces a disjoint class set with the same domains. 2) DIL only considers domain variation, where each incremental task introduces a different domain while sharing the same class set. However, both types simplify the IL scenario by concentrating on a single type of increment (i.e., either increasing new classes or domains), limiting their applicability. Actually, various types of increments across task distributions often arrive randomly in the unpredictable wild. For instance, the discovery of unknown classes frequently coincides with new domains due to varying weather conditions in realistic road scenes [22, 24]. More recently, Versatile Incremental Learning (VIL) [26] has been proposed to simulate the class- and domain-agnostic IL scenario without prior knowledge of which new classes or domains would increase, as illustrated in Fig. 1. However, VIL assumes that the scale of these increments (i.e., the number of new classes or domains) is static, which still significantly differs from dynamic reality where the scale of a new task is constantly changing. To relax these assumptions, it is necessary to explore a more general incremental learning scenario that simultaneously considers the randomness of incremental task types across all task distributions and the scale of increments within each task distribution. Such a scenario better reflects real-world conditions.

In this paper, we investigate a new IL scenario called **Universal Incremental Learning (UIL)**, as illustrated in Fig. 1. In UIL, each incoming task has a random type of increments, which may involve new classes with previous domains, new domains with previous classes, or entirely new classes with new domains. Moreover, the scale of these increments is also random. The word “universal” indicates that UIL has no prior knowledge of both the type and scale of increments for each incoming task. In UIL, it poses two significant challenges for existing IL methods: 1) Since incremental types vary randomly across all task distributions, designing specific learnable modules tailored to a single type, as in existing IL methods [37–39], becomes ineffective. Moreover, when the model encounters a new incremental type, it will learn conflicting knowledge compared to what has already acquired in previous tasks, hindering accurate and deterministic predictions and thus causing catastrophic forgetting. We refer to this challenge as *inter-task distribution confusion* arising from random incremental types. 2) Given the random scale of increments within each task distribution, the class distribution evolves inherently imbalanced due to various emerging frequencies in the dynamic wild. Standard optimization algorithms [14, 16] calculate the average loss on all samples and update the parameters accordingly. However, a major challenge in training on imbalanced class distribution is asymmetrical opti-

mization: gradient updates favor head classes with more samples, making the average gradient updates detrimental to tail classes with fewer samples. Consequently, tail classes easily suffer from under-fitting while head classes over-fit. We refer to this challenge as *intra-task distribution confusion* arising from random incremental scale.

To address the challenges of our UIL, we propose a simple yet effective method named **MiCo**, which individually **Mitigating Confusion** arising from inter- and intra-task distribution randomness. This method employs a multi-objective learning scheme and introduces direction- and magnitude-decoupled recalibration modules. Specifically, cross-entropy loss \mathcal{L}_{ce} guides the model to distinguish correct labels by narrowing the distribution gap between prediction and ground truth, while entropy minimization loss \mathcal{L}_{em} [25, 35] encourages the model to make deterministic predictions via explicitly reducing the prediction distribution entropy (PDE) of the samples, contributing to accurate and deterministic predictions regardless of how the incremental type changes. With the favor of reducing conflicting gradients (i.e. gradient cosine similarity (GCS) $\cos \theta < 0$) in the direction recalibration module, the effectiveness of multi-objective learning scheme is further enhanced. In addition, asymmetrical optimization towards imbalanced class distribution is alleviated via the magnitude recalibration module, based on a high positive relationship between class distribution and gradient magnitude for each class. Overall, our main contributions are highlighted as follows:

1. We investigate a more general and realistic IL scenario than existing ones called Universal Incremental Learning (UIL), by simultaneously considering randomness in the type and scale of increments.
2. A simple yet effective framework named MiCo is proposed to mitigate confusion arising from inter- and intra-task distribution randomness in UIL, respectively.
3. Extensive experiments on three benchmarks demonstrate that our MiCo outperforms existing state-of-the-art methods in both the proposed UIL scenario and the existing VIL scenario.

2. Related Work

2.1. Incremental Learning

Incremental Learning (IL) faces the core challenge of overcoming catastrophic forgetting. This phenomenon refers to the model’s tendency to forget previously learned knowledge while acquiring new knowledge. To address this issue, numerous methods have been proposed. For example, rehearsal-based methods [8, 12, 13, 21] alleviate forgetting by replaying real or synthetic samples from previous tasks. These methods include experience replay [8, 21], which utilizes stored experiences from a memory buffer, and generative replay [12, 13], where a generative model creates syn-

thetic data to simulate previous knowledge. Regularization-based methods maintain a relative balance between stability and plasticity during the learning of new tasks. Representative methods [15, 26, 42] involve designing the regularization loss that protects important parameters, ensuring that the model retains crucial information from earlier tasks while adapting to new ones. With the rise of tuning pre-trained models [11, 17, 43], prompt-based methods [33, 38, 39] have emerged as a promising alternative for IL. By injecting a small set of learnable parameters, these methods prompt the model to acquire additional instructions, enabling it to learn both task-specific and task-agnostic knowledge throughout a sequence of tasks.

2.2. Entropy Minimization

Entropy minimization, serving as a crucial regularizer, has been widely studied to improve generalization against domain shift in domain adaptation [30, 31] and test-time adaptation [35, 41]. Moreover, in the context of semi-supervised learning [1], entropy minimization is employed to enhance the robustness of models against random appearance variation. These methods demonstrate that reducing entropy can achieve excellent performance on out-of-distribution and unknown data. Our UIL confuses the model with random incremental types (i.e. ever-varying classes and domains) across all task distributions, so entropy minimization is an explicit solution to mitigate this confusion.

2.3. Optimization for Incremental Learning

Optimization-based methods for IL [2, 5, 8, 20, 32, 36] manipulate gradient direction to overcome catastrophic forgetting. For example, existing methods [2, 20] constrain the gradient direction of new tasks to align with the rehearsals' direction, ensuring consistency in gradient spaces. GPM [32] and OGD [5] share similarities in preserving the gradient direction of the current task relative to previous tasks through explicit gradient projection and rectification, respectively. DGR [8] focuses on rectifying the gradient magnitude for each class while constraining parameter updates by distillation rehearsal's distribution to preserve the learned knowledge. However, these optimization-based methods struggle in random task distributions. Constraining gradient direction to previous tasks causes significant forgetting due to inherent direction variation in a dynamically varying IL scenario [26].

3. Universal Incremental Learning

3.1. Problem Formulation and Definition

Problem Formulation. We formally introduce the definition of Universal Incremental Learning (UIL). Let $\mathcal{D} = \{D_1, D_2, \dots, D_T\}$ denote a sequence of T disjoint tasks. Each task $D_t = \{\mathcal{X}_t, \mathcal{Y}_t\}$ contains n_t images $\mathcal{X}_t =$

$\{x_1, x_2, \dots, x_{n_t}\}$ and the corresponding labels $\mathcal{Y}_t = \{y_1, y_2, \dots, y_{n_t}\}$. For $i \in [1, 2, \dots, n_t]$, each label $y_i = (c_i, m_i)$ is annotated with the class label $c_i \in \mathcal{C}_t$ and the domain label $m_i \in \mathcal{M}_t$. Formally, for $t, t' \in [1, 2, \dots, T]$, disjoint tasks without overlapping samples can be expressed as $\mathcal{X}_t \cap \mathcal{X}_{t'} = \emptyset$ and $\mathcal{Y}_t \cap \mathcal{Y}_{t'} = \emptyset$ for $t \neq t'$. UIL aims to simultaneously consider randomness from the type and scale of increments. Therefore, the size of the class set \mathcal{C}_t and the domain set \mathcal{M}_t , represented by $|\mathcal{C}_t|$ and $|\mathcal{M}_t|$, are random. The model f_T^θ parameterized by θ_T at task T is only trained on training set $D_{train} = D_T$ but is evaluated on test set $D_{test} = \{D_1, D_2, \dots, D_T\}$ to achieve overall performance across T tasks. To achieve this, the model is trained using the following objective, as shown in Eq. 1:

$$\mathcal{L}_\theta = \sum_{t=1}^T \mathbb{E}_{x, y \sim \mathcal{X}_t, \mathcal{Y}_t} L(f_t^\theta(x), y), \quad (1)$$

where L is a common cross-entropy loss for classification.

In terms of $|\mathcal{C}_t|$ and $|\mathcal{M}_t|$ at task t , the universality of our proposed UIL is evident in the fact that the VIL scenario is actually a special case of the UIL scenario when $|\mathcal{C}_t| = C$ and $|\mathcal{M}_t| = 1$, where C is a static constant.

Definition 3.1 (Prediction Distribution Entropy, PDE). At task t , we denote $\hat{y}_{i,c}$ as the logits of the i -th sample x_i at c -th class index, predicted by the model f_t^θ . $p(\hat{y}_{i,c})$ is corresponding probability after softmax operation. The PDE of x_i is defined in Eq. 2:

$$H(y_i) = - \sum_{c=0}^{|\mathcal{C}_t|} p(\hat{y}_{i,c}) \log p(\hat{y}_{i,c}). \quad (2)$$

As shown in Eq. 3, the output probability $p(\hat{y}_i)$ follows a uniform distribution, indicating complete confusion in its ability to discriminate among \mathcal{C}_t , with highest value $\log |\mathcal{C}_t|$. Conversely, when the output probability $p(\hat{y}_i)$ follows a one-hot distribution, reflecting a fully deterministic prediction, with the lowest value 0.

$$0 \leq H(y_i) \leq \log |\mathcal{C}_t|. \quad (3)$$

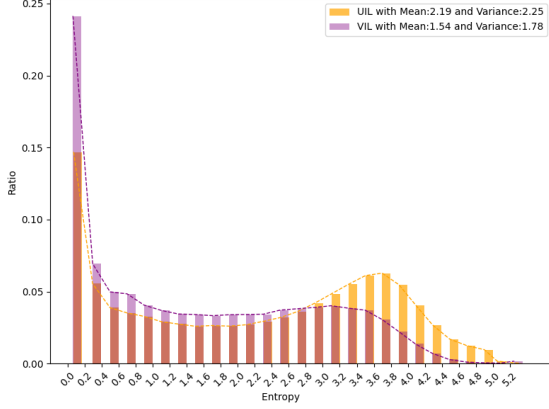
Definition 3.2 (Gradient Cosine Similarity, GCS). Denote $\theta_{u,v}$ as the angle between two gradients g_u and g_v . GCS is denoted as $\cos \theta_{u,v}$ between g_u and g_v , as shown in Eq. 4:

$$\cos \theta_{u,v} = \frac{g_u}{\|g_u\|} \cdot \frac{g_v}{\|g_v\|}, \quad (4)$$

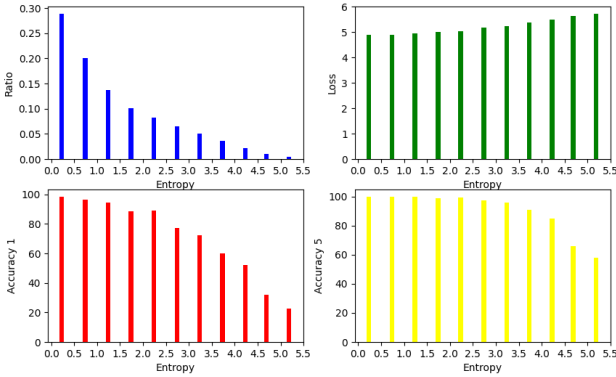
where the conflicting gradients occur when $\cos \theta_{u,v} < 0$.

3.2. Challenge Analysis

To analyze the challenges of our UIL, we perform a detailed investigation. **At the inter-task distribution level**, we individually calculate PDE of all test samples in the UIL and VIL scenario after incremental training on the same



(a) Distribution comparison of prediction distribution entropy (PDE) between UIL and VIL scenarios. Our UIL causes more confusion to the model than VIL with larger entropy mean and variance (i.e. 2.19 vs 1.54 and 2.25 vs 1.78), due to the smaller proportion of samples in the low-entropy intervals and the larger proportion in the high-entropy intervals.



(b) Distributions on entropy, test loss, and test accuracy are analyzed. We randomly sample a dataset from our UIL scenario and categorize the samples into entropy intervals. The results, including the ratio of each interval, along with the average loss and average accuracy during the inference phase, indicate that lower entropy lead to higher accuracy.

Figure 2. Analysis on entropy distribution in the proposed UIL scenario, as well as the VIL scenario.

$T = 30$ tasks using the dataset [27] with various classes and domains. Then we divide all test samples into multiple intervals based on $H(y_i)$ in ascending order, such as $\mathcal{I} = \{\mathcal{I}_1, \mathcal{I}_2, \mathcal{I}_3, \dots, \mathcal{I}_{27}\}$, and count the ratio of samples in each interval to all samples. As illustrated in Fig. 2a, the UIL scenario results in more confusion than the VIL scenario, as proved by two key observations: 1) The ratio of samples in the low-entropy intervals is significantly smaller. 2) The ratio of samples in the high-entropy intervals is relatively larger. Besides, Fig. 2b indicates that lower entropy samples lead to more accurate predictions, suggesting that reducing entropy distribution is an effective way to improve model accuracy.

At the intra-task distribution level, during training

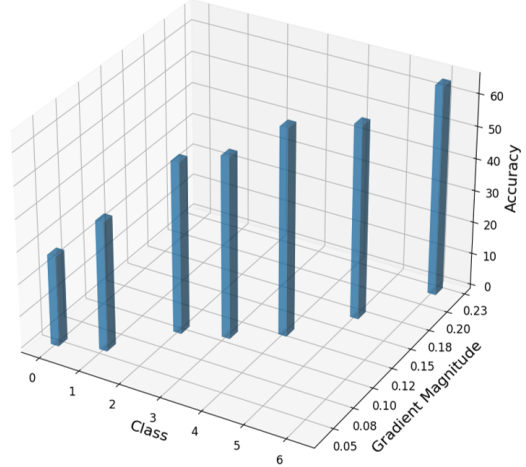


Figure 3. Illustration on the joint relationship among classes, corresponding gradient magnitude and test accuracy in a 3D bar chart. The imbalanced class distribution are resorted in ascending order based on the number of samples. This figure indicates that there is positive trend where higher gradient magnitudes correlate with improved accuracy, offering valuable insights into the performance across different classes.

phase, we calculate the average gradient magnitudes of the corresponding class’s weight vectors across three random experiments. In addition, the average test accuracy of corresponding classes is computed during inference phase. The joint relationship among the classes, gradient magnitude and test accuracy is illustrated in Fig. 3. We observe a positive trend that the larger gradient magnitude is significantly associated with higher accuracy. This causes the model to learn knowledge from head classes in a biased manner if no any intervention is given, referred to asymmetrical optimization. Consequently, the model is confused about tail classes and biased to predict head classes, failing to achieve comprehensive performance across classes.

4. Method

Inspired by these observations in Sec. 3, we propose a simple yet effective framework for the UIL scenario, named MiCo. As illustrated in Fig. 4, the architecture of MiCo consists of a frozen pre-trained model and a trainable classifier during training on $\mathcal{D}_{train} = \mathcal{D}_t$, and all parameters are frozen during evaluation on previous tasks $\mathcal{D}_{test} = \{\mathcal{D}_1, \dots, \mathcal{D}_t\}$. In Sec. 4.1, to mitigate confusion from inter-task distribution randomness, we firstly employ a multi-objective learning scheme, referred to joint training using \mathcal{L}_{ce} and \mathcal{L}_{em} , to enforce the model to produce accurate and deterministic predictions for random IL types across all task distributions. Furthermore, we introduce a direction recalibration module to enhance its effectiveness by reducing conflicting gradients, referred to $\tilde{g}_{ce} = \frac{g_{ce}}{\|g_{ce}\|}$

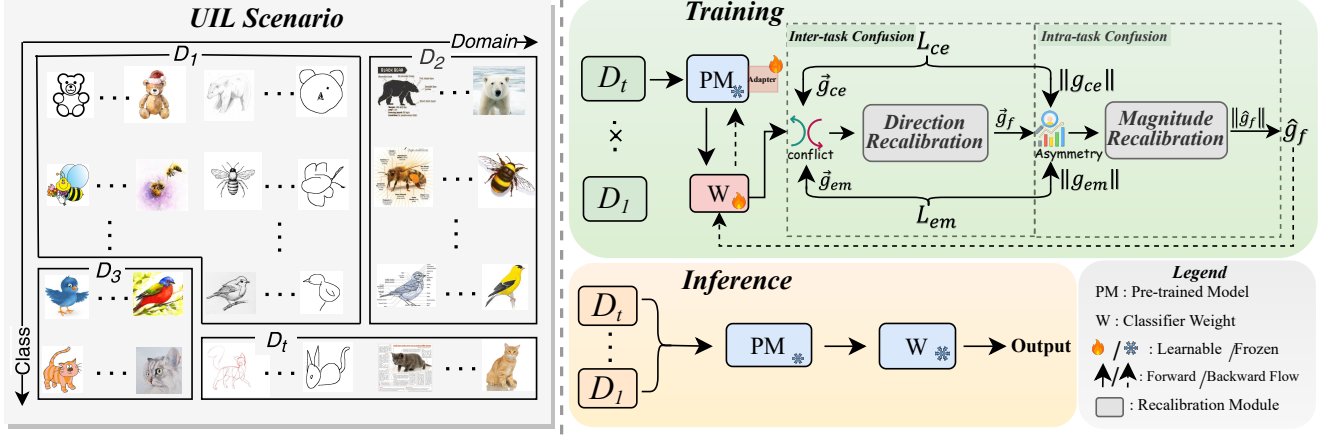


Figure 4. Overview of our proposed UIL scenario (left) and our framework MiCo (right). During training on $\mathcal{D}_{train} = \mathcal{D}_t$, MiCo employs a multi-objective learning scheme and introduces direction- and magnitude-decoupled recalibration modules to mitigate confusion from inter- and intra-task distribution randomness. \mathcal{L}_{ce} and \mathcal{L}_{em} jointly enforce the model to make accurate and deterministic predictions with the role of reducing conflict between \vec{g}_{ce} and \vec{g}_{em} via a direction recalibration module. Moreover, a magnitude recalibration module is used to rescale gradient magnitude (e.g., $\|\vec{g}_{ce}\|$ and $\|\vec{g}_{em}\|$), aiming to alleviate asymmetrical optimization towards imbalanced class distribution. Finally, gradient \hat{g}_f with recalibrated direction \vec{g}_f and magnitude $\|\hat{g}_f\|$ is used to update parameters in backward propagation. During inference, all previous tasks $\mathcal{D}_{test} = \{D_1, \dots, D_t\}$ are evaluated.

and $\vec{g}_{em} = \frac{\vec{g}_{em}}{\|\vec{g}_{em}\|}$. In Sec. 4.2, we introduce how to mitigate confusion from intra-task distribution randomness. Towards training on imbalanced class distribution, we introduce a magnitude recalibration module to alleviate the challenge of asymmetrical optimization via rescaling gradient magnitude, referred to $\|\vec{g}_{ce}\|$ and $\|\vec{g}_{em}\|$. The gradient \hat{g}_f after recalibration is finally used to update parameters in backward propagation.

4.1. Mitigating Confusion from Inter-task Distribution Randomness

In the CIL or DIL scenario, the incremental tasks have class- or domain- priority. Specifically, only the same number of new classes or domains, are sequentially introduced, allowing the model to confidently learn class- or domain-specific knowledge. However, there is no prior knowledge of the incremental type in the proposed UIL scenario. As a result, it confuses the model that the new knowledge introduced by new incremental types conflicts with that it has already learned, leading to confused prediction towards previous tasks. To address this, we employ a multi-objective learning scheme, which guide the model to make accurate and consistent predictions in confused IL scenarios.

As shown in Fig. 4, we joint train the model using the cross-entropy loss \mathcal{L}_{ce} and the entropy minimization (EM) loss \mathcal{L}_{em} , which is commonly used in test-time adaptation [25, 35]. Specifically, we treat $p(\hat{y}_{i,c})$ as the probability that the input sample x_i is classified as c -th label, where $\hat{y}_{i,c}$ is logits at the c -th position of the model’s output. The prediction distribution entropy (PDE) of x_i is $H(y_i)$, as shown

in Eq. 2. Across all task distributions with random incremental types, given to the sample x_i with the random label y_i , we guide the model to make accurate and deterministic predictions by teaching to correctly distinguish ground-truth label and explicitly reducing its PDE. Overall, MiCo is trained using the following multi-objective loss \mathcal{L} , as shown in Eq. 5:

$$\mathcal{L} = \mathcal{L}_{ce} + \gamma \cdot \mathcal{L}_{em}, \quad (5)$$

where γ is balanced coefficient, discussed in ablation study as shown in Table. 3.

To enhance the effectiveness of the multi-objective learning scheme, the direction recalibration module is introduced to reduce the conflicting gradients between \vec{g}_{ce} and \vec{g}_{em} . This is based on the observation that the gradient cosine similarity (GCS) is negative. Specifically, denote $\mathcal{G}_d = \{\vec{g}^1, \vec{g}^2, \dots, \vec{g}^c\}$ as the set of gradient direction, where c individually the class index of c -th weight vector in the classifier. As shown in Eq. 6:

$$\begin{aligned} \vec{g}^c &= \vec{g}_{ce}^c + \gamma \cdot \vec{g}_{em}^c, \\ \vec{g}_f^c &= \vec{g}^c + \beta \cdot \vec{g}_w^c, \end{aligned} \quad (6)$$

where γ is the same coefficient as Eq. 5 and \vec{g}^c is original gradient direction before the direction recalibration module. $\beta = f(\|\vec{g}^c\|)$ is constant to c -th index and \vec{g}_w^c is the recalibration offset, which can be solved in dual optimization, referred to [18]. Finally, \vec{g}_f^c is the gradient direction of classifier’s c -th weight vector after the direction recalibration module. As a result, with the multi-objective learning scheme and the avoidance of conflicting gradient in the di-

rection module, our model achieves not only accurate and deterministic predictions but also learns in a conflict-free direction, regardless of the variation in incremental types.

4.2. Mitigating Confusion from Intra-task Distribution Randomness

In the dynamic wild, the scale of these increments (i.e. the number of classes) is random, so the class distribution is eventually imbalanced due to distinct emergent frequencies. The standard optimization algorithm [14, 16] is to calculate the average loss across samples in a mini-batch and update parameters accordingly, regardless of whether class distribution is balanced or not. We identify a major challenge towards training on imbalanced class distribution, named asymmetrical optimization, where the classifier’s weight vectors corresponding to head classes experience substantial updates due to larger gradient magnitudes than tail classes.

To address this, we introduce a magnitude recalibration module to alleviate the asymmetrical optimization by rescaling the classifier’s gradient magnitude. Specifically, denote $\mathcal{G}_m = \{\|g^1\|, \|g^2\|, \dots, \|g^c\|\}$ as the set of gradient magnitude, where c is the class index of c -th weight vector. $\|g^c\|$ is defined in Eq. 7:

$$\|g^c\| = \|g_{ce}^c + \gamma \cdot g_{em}^c\|, \quad (7)$$

where g_{ce}^c and g_{em}^c are gradient vector from \mathcal{L}_{ce} and \mathcal{L}_{em} , respectively. $\|g^c\|$ is the accumulated gradient magnitude after vector summation. γ is the same balanced coefficient as Eq.5. We rescale each gradient magnitude in \mathcal{G}_m using class-specific factor w derived from Min-Max Normalization on \mathcal{G}_m . As shown in Eq. 8:

$$\begin{aligned} \|\hat{g}^c\| &= w_c * \|g^c\|, \\ \text{where } w_c &= 1 - \frac{\|g^c\| - \min(\mathcal{G}_m)}{\max(\mathcal{G}_m) - \min(\mathcal{G}_m)}. \end{aligned} \quad (8)$$

Finally, the recalibrated gradient \hat{g}_f^c with direction \vec{g}_f^c and magnitude $\|\hat{g}_f^c\|$, as shown in Eq.6 and Eq.8, is used to update the classifier’s c -th weight in backward propagation. With the magnitude calibration module, our model effectively alleviates asymmetrical optimization by simple rescaling strategy when faced with imbalanced class distribution, allowing it to fairly acquire knowledge without learning bias, thereby achieving comprehensive performance across all classes.

5. Experiments

In this section, we conduct extensive experiments for comparison with state-of-the-art methods. First, we describe the experiment setup including datasets, evaluation metrics and comparison methods in Sec. 5.1. Moreover, we present the

Table 1. Task configuration on three benchmarks in the UIL and VIL scenario. $T, \|\mathcal{C}_t\|$ and $\|\mathcal{M}_t\|$ denote the total number of sequential tasks, the number of classes and the number of domains within each incremental task, respectively. In the UIL scenario, *unk* indicates that the number of classes and domains are unknown due to random scale of these increments. The value with asterisk (*) indicates that we try to ensure that each task covers multiple domains, preventing the UIL scenario from degrading into the VIL scenario for iDigits with fewer classes and domains, which leads to fewer tasks overall.

Dataset	VIL			UIL		
	T	$\ \mathcal{C}_t\ $	$\ \mathcal{M}_t\ $	T	$\ \mathcal{C}_t\ $	$\ \mathcal{M}_t\ $
iDigits [34]	20	2	1	5*	<i>unk</i>	<i>unk</i>
CORe50 [19]	40	10	1	40	<i>unk</i>	<i>unk</i>
DomainNet [27]	30	10	1	30	<i>unk</i>	<i>unk</i>

experimental results to demonstrate the superiority of our approach in Sec. 5.2. Finally, the effectiveness of each component is verified through ablative studies in Sec. 5.3.

5.1. Experiment Setup

Datasets and Metrics. Following the previous methods [7, 23, 26, 39], our experiments are conducted on datasets with various classes and domains: iDigits [34], CORe50 [19], DomainNet [27], which can easily be investigated in the realistic UIL and VIL scenario. The detailed task configuration is described in Table. 1. As previous evaluation protocol in [26, 33, 38, 39], we report the performance after training the last task T using commonly evaluation metrics: average accuracy (marked as Avg. Acc) and forgetting rate (marked as Forgetting). Besides, due to the randomness causing an imbalanced data distribution across task distributions, we also report the weighted accuracy (marked as W. Acc) on all tasks for a comprehensive evaluation, where each task’s accuracy is averaged by the weight of each task.

Comparison Methods and Implementation Details. We compare MiCo with the state-of-the-art IL methods of three categories: prompt-based methods [33, 37–39], regularization-based methods [8, 26], mixture-based methods [7]. In addition, we also conduct the fine-tuning and joint-training experiments to provide the lower bound and upper bound of performance in a linear probe way [9, 10, 28]. All IL methods uniformly use ViT-B/16 [4] as the pre-trained backbone. Each method is trained over three random experiments with different seeds, and we report final performance as the mean and standard deviation. For training configuration (i.e., learning rate, epochs and learnable adapter for fine-tuning backbone), we keep the same setting as ICON [26].

Table 2. Comparison with state-of-the-art IL methods on the UIL and VIL scenario. The comparison is shown in terms of Avg. Acc(\uparrow), W. Acc(\uparrow), and Forgetting(\downarrow) as the mean and standard deviation across three random experiments. The Avg. Acc(\uparrow) on both scenarios is averaged as the Mean Acc(\uparrow) at the last column. Since joint training, as the *upper-bound* performance, is inherently scenario-agnostic for incremental learning, so the only Avg. Acc(\uparrow) is reported. For a comprehensive comparison, we compare MiCo with recently existing methods of prompt-based [33, 38, 39], mixture-based [7] and regularization-based [8, 26]. We maintain a fixed amount of memory with 10 samples per classes for replaying experiences in [8]. The best and second results are marked in the **bold** and underline, respectively.

Method	VIL			UIL			Mean Acc(↑)
	Avg. Acc(↑)	W. Acc(↑)	Forgetting(↓)	Avg. Acc(↑)	W. Acc(↑)	Forgetting(↓)	
iDigits							
Upper-bound			-				95.6±0.4
Lower-bound	36.3±0.1	32.6±1.0	21.5±5.5	46.5±0.5	50±2.4	18.4±13.0	41.4±0.3
L2P [39]	57.2±3.0	52.1±3.7	32.1±4.1	74.3±1.3	74.1±3.0	18.0±9.1	65.8±2.2
DualPrompt [38]	61.8±1.5	59.0±2.9	24.9±3.6	74.3±0.1	75.4±0.4	15.4±4.5	68.1±0.8
CODA-Prompt [33]	64.6±1.8	61.0±3.5	23.6±1.7	79.0±11.2	78.0±12.7	18.3±17.0	71.8±6.5
DGR [8]	65.3±3.2	63.9±2.6	38.0±3.7	79.3±4.9	77.6±8.1	25.4±5.3	72.3±4.1
LAE [7]	50.1±4.3	42.5±5.4	36.1±1.0	74.5±2.2	74.4±1.6	21.7±2.0	62.3±3.3
ICON [26]	68.0±2.0	65.1±2.5	21.3±2.7	81.8±8.0	80.2±10.3	15.7±13.1	74.9±5.0
Ours: MiCo	69.5±3.2	67.3±3.5	23.4±5.4	84.6±4.1	83.9±6.2	11.5±4.3	77.1±3.6
CORe50							
Upper-bound			-				95.3±0.3
Lower-bound	69.6±0.3	69.6±0.4	5.9±0.8	45.1±4.0	46.4±4.4	16.8±0.2	57.4±2.2
L2P [39]	75.5±3.5	75.6±3.5	8.0±1.9	50.0±1.6	51.6±0.9	18.6±2.9	62.8±2.6
DualPrompt [38]	73.1±7.6	73.1±7.6	9.8±4.3	51.4±1.6	52.6±1.0	18.1±3.0	62.3±4.6
CODA-Prompt [33]	73.2±0.1	73.3±0.2	8.0±2.0	53.9±2.3	54.2±1.5	15.7±5.4	63.6±1.2
DGR [8]	77.5±3.3	77.0±2.9	12.4±3.8	55.8±3.6	56.7±2.4	20.1±3.5	66.7±3.5
LAE [7]	72.0±3.2	73.2±2.6	8.3±2.7	54.1±5.0	55.5±5.4	16.6±1.0	63.1±4.1
ICON [26]	80.6±1.1	80.7±1.0	6.2±0.1	57.5±1.2	59.1±1.1	15.8±4.4	69.1±1.2
Ours: MiCo	83.5±0.8	82.0±0.8	5.3±0.5	67.4±2.3	66.4±2.0	16.4±3.2	75.5±1.5
DomainNet							
Upper-bound			-				59.5±0.4
Lower-bound	42.0±2.8	43.4±1.5	15.2±1.9	42.1±3.6	45.9±0.2	8.3±2.8	42.1±3.2
L2P [39]	47.0±1.7	47.3±1.2	24.2±1.7	43.2±0.9	41.6±0.7	22.4±4.9	45.1±1.3
DualPrompt [38]	45.8±2.9	47.1±1.2	18.6±2.7	46.3±3.4	42.0±1.9	23.5±5.0	46.1±3.2
CODA-Prompt [33]	47.6±1.9	48.4±0.8	19.9±1.7	46.0±2.4	43.2±1.9	24.2±3.5	46.8±2.2
DGR [8]	48.3±1.5	48.8±1.4	19.6±2.2	49.2±3.0	50.1±1.8	23.4±3.8	48.8±2.3
LAE [7]	44.6±0.5	43.8±1.2	25.0±2.3	47.5±3.1	42.1±1.9	19.3±4.9	46.1±1.8
ICON [26]	49.8±0.3	52.6±1.7	14.4±1.3	52.3±2.6	53.0±1.5	15.2±2.6	51.1±1.5
Ours: MiCo	52.3±1.2	56.7±1.3	16.7±1.5	55.2±2.3	56.1±0.1	15.0±2.8	53.8±1.8

Table 3. Ablation experiments of each component in UIL. *mobj* is the multi-objective learning scheme. *dir* is the direction recalibration module. *mag* is the magnitude recalibration module. \checkmark indicates the component is enables. We conduct ablative experiments by progressively integrating each component into the baseline from baseline (1) to MiCo (6). *dir* only exists in conjunction with *mobj*, aiming to reduce conflicting gradients. The Avg. Acc(\uparrow) across three benchmarks is averaged as the Mean Acc(\uparrow) at the last column.

ID	Method			iDigits			CORe50			DomainNet			Mean Acc(\uparrow)
	<i>mobj</i>	<i>dir</i>	<i>mag</i>	Avg. Acc(\uparrow)	W. Acc(\uparrow)	Forgetting(\downarrow)	Avg. Acc(\uparrow)	W. Acc(\uparrow)	Forgetting(\downarrow)	Avg. Acc(\uparrow)	W. Acc(\uparrow)	Forgetting(\downarrow)	
(1)				78.3 \pm 3.2	79.5 \pm 6.1	14.3 \pm 7.9	64.9 \pm 5.6	64.7 \pm 6.9	20.5 \pm 4.3	46.9 \pm 3.8	55.2 \pm 1.4	11.6 \pm 2.6	63.3 \pm 4.2
(2)	\checkmark			80.4 \pm 4.6	81.0 \pm 5.9	13.5 \pm 9.5	65.0 \pm 3.2	65.5 \pm 4.4	19.7 \pm 2.3	49.8 \pm 3.0	55.7 \pm 1.4	16.6 \pm 1.4	65.1 \pm 3.6
(3)			\checkmark	81.3 \pm 4.4	82.4 \pm 6.3	13.0 \pm 9.1	65.9 \pm 3.8	65.9 \pm 4.6	18.3 \pm 4.2	50.2 \pm 3.1	54.5 \pm 1.4	14.9\pm1.9	65.8 \pm 3.7
(4)	\checkmark		\checkmark	84.0 \pm 3.0	83.9 \pm 4.7	12.4 \pm 6.9	67.1 \pm 2.5	66.9\pm2.1	17.1 \pm 2.8	53.1 \pm 2.6	55.9 \pm 0.3	14.5 \pm 0.7	68.1 \pm 2.7
(5)	\checkmark	\checkmark		83.1 \pm 3.9	82.5 \pm 6.0	13.4 \pm 7.4	66.4 \pm 1.2	67.3 \pm 2.3	19.0 \pm 2.3	51.2 \pm 3.1	55.2 \pm 0.3	15.8 \pm 5.1	67.0 \pm 2.7
(6)	\checkmark	\checkmark	\checkmark	84.6\pm4.1	83.9\pm6.2	11.5\pm4.3	67.4\pm2.3	66.4 \pm 2.0	16.4\pm3.2	55.2\pm2.3	56.1\pm0.1	15.0 \pm 2.8	69.1\pm2.9

Table 4. Ablation of γ in UIL. The Avg. Acc(\uparrow) across three benchmarks is averaged as the Mean Acc(\uparrow) at the last column.

γ	iDigits			COr50			DomainNet			Mean Acc(\uparrow)
	Avg. Acc(\uparrow)	W. Acc(\uparrow)	Forgetting(\downarrow)	Avg. Acc(\uparrow)	W. Acc(\uparrow)	Forgetting(\downarrow)	Avg. Acc(\uparrow)	Avg. Acc(\uparrow)	Forgetting(\downarrow)	
1.0	85.1\pm4.3	84.0\pm 5.3	12.7 \pm 7.9	66.3 \pm 3.4	66.6 \pm 2.8	17.2 \pm 2.1	47.3 \pm 3.9	54.4 \pm 0.5	11.1 \pm 1.7	66.2 \pm 3.9
0.1	80.5 \pm 7.9	80.8 \pm 8.4	15.8 \pm 10.2	66.5 \pm 4.5	66.4 \pm 5.6	17.8 \pm 5.2	52.0 \pm 1.2	55.5 \pm 0.7	15.3 \pm 4.9	66.3 \pm 4.5
0.01	84.6 \pm 4.1	83.9 \pm 6.2	11.5\pm4.3	67.4\pm2.3	66.4\pm2.0	16.4\pm3.2	55.2\pm2.3	56.1\pm0.1	15.0\pm2.8	69.1\pm2.9
0.001	83.2 \pm 2.1	82.1 \pm 5.8	13.6 \pm 7.6	66.5 \pm 2.1	66.2 \pm 0.3	22.0 \pm 0.6	52.0 \pm 0.1	54.9 \pm 0.1	19.1 \pm 1.3	67.2 \pm 1.4

5.2. Comparison with State-of-The-Art IL Methods

We compare MiCo with the existing method in realistic IL scenarios, including the proposed UIL scenario and the VIL scenario. As shown in Table. 2, MiCo significantly outperforms existing sota methods in general UIL and VIL scenario in terms of all evaluation metrics. Compared with second results of 74.9, 69.1, 51.1 in terms of Mean Acc (\uparrow) on three benchmarks, our MiCo achieves significant gains with **77.1 (+2.2)**, **75.5 (+6.4)**, **53.8 (+2.7)** and simultaneously has comparable variance with **3.6 (-1.4)**, **1.5 (+0.3)**, **1.8 (+0.3)** in the corresponding benchmarks. Moreover, the ability of MiCo to overcome catastrophic forgetting also maintains a considerable mean Forgetting (\downarrow) with the second place [26]. These observations demonstrate that MiCo has a more robust ability to mitigate confusion from inter- and intra-task distribution randomness without degrading the ability to overcome forgetting. Existing prompt-based methods L2P[39], DualPrompt [38], CODA-Prompt [33] aim to select generalizable prompts by utilizing a cosine similarity-based matching mechanism to mitigate catastrophic forgetting without storing previous rehearsal. It is ineffective when domain variation continually occurs within classes in the UIL scenario, because similarity-based matching is extremely sensitive to appearance variation. Among regularization-based methods, ICON [26] introduces specific regularization terms by enforcing orthogonality among adapter shifts to alleviate forgetting but shows suboptimal performance due to random incremental scales. DGR [8] relies on the prior distribution of the stored rehearsals to distill the previous knowledge but gets confused about varying incremental types. LAE [7], a representative mixture-based method, continually merges online and offline models into one unified model to overcome forgetting. However, its performance is not unstable in the more confused IL scenario. Instead, the results in Table. 2 indicates that our MiCo achieves reliable performance in both scenarios. Actually, our UIL inevitably involves knowledge overlap across all tasks (i.e. the former and the latter tasks share the same classes or domains). Therefore, vanilla fine-tuning even without any specific architectures can performs well.

5.3. Ablation Study

Effectiveness of Components. As shown in Table. 3, we conduct ablative experiments by progressively integrating

each component into our baseline to verify the effectiveness of each component. Compared with Mean Acc (\uparrow) of 63.3 \pm 4.2 of baseline (1), the effectiveness of the multi-objective learning scheme in (2) is validated, achieving significant gains with **65.1 \pm 3.6** and surpassing the baseline by **1.8** points. The results demonstrate that the multi-objective learning scheme contributes to making accurate and deterministic predictions regardless of random incremental types across all task distributions. Additionally, the effectiveness of the magnitude recalibration module in (3) is verified, achieving significant gains with **65.8 \pm 3.7** and surpass the baseline by **2.5** points. The results demonstrate that the magnitude recalibration module could effectively alleviate asymmetrical optimization towards imbalanced class distribution. By simultaneously adopting the multi-objective learning scheme and the magnitude recalibration module in (4), the effectiveness of each component can be leveraged through synergy, achieving absolute gains up to **3.0** and **2.3** points, respectively. To ablate the direction recalibration module, we combine the multi-objective learning with the direction recalibration module in (5) and (6), respectively. The effectiveness of the multi-objective learning scheme is further enhanced. Although our direction calibration module indirectly modifies the gradient magnitude, there is synergistic when simultaneously enabling direction- and magnitude-decoupled recalibration modules, indicated by the comparison of (4), (5) and (6). Overall, each component of our MiCo (6) is cooperative and effective in improving accuracy and overcoming forgetting for the UIL scenario, outperforming the baseline (1) with accuracy gains up to **5.8** points and forgetting gains down to **1.2** points.

Ablation of γ . In our multi-objective learning scheme, we perform three random experiments with different seeds to find the best γ , i.e. $\gamma \in \{1.0, 0.1, 0.01, 0.001\}$. As shown in Table.4, when γ set to 0.01, it exhibits the best performance at the peak on both COr50 [19] and DomainNet [27], particularly in terms of Avg. Acc(\uparrow). Although $\gamma = 0.01$ fails to achieve the best accuracy on iDigits [34], it has comparable performance in terms of accuracy and the best performance in terms of forgetting. The results indicate that excessively larger values can lead to degrading accuracy, while excessively small values are unable to make deterministic predictions. Therefore, γ is set to 0.01 by default in our experiments.

6. Conclusion

In this paper, we investigate a more general and realistic Universal Incremental Learning (UIL), where the model has no prior knowledge of the types and scale of increments. Furthermore, we conduct the detailed analysis for the UIL scenario and identify confusion arising from inter- and intra-task distribution randomness. To mitigate confusion, we propose a simple yet effective framework named MiCo, consisting of a multi-objective learning scheme and direction- and magnitude-decoupled recalibration modules. Extensive experiments demonstrate that our MiCo shows sota performance on the UIL scenario, and existing VIL scenario. We hope that UIL could provide new insights for IL community. In the future, our focus will be on establishing a comprehensive benchmark for UIL to accurately measure performance.

Acknowledgement

This work was supported by the National Natural Science Foundation of China (Nos.62476054, and 62172228).

References

- [1] David Berthelot, Nicholas Carlini, Ian Goodfellow, Nicolas Papernot, Avital Oliver, and Colin Raffel. Mixmatch: A holistic approach to semi-supervised learning. *arXiv preprint arXiv:1905.02249*, 2019. 3
- [2] Arslan Chaudhry, Marc’Aurelio Ranzato, Marcus Rohrbach, and Mohamed Elhoseiny. Efficient lifelong learning with a gem. In *ICLR*, 2019. 3
- [3] Wei Chen and Yi Zhou. Make domain shift a catastrophic forgetting alleviator in class-incremental learning. *arXiv preprint arXiv:2501.00237*, 2024. 1
- [4] Alexey Dosovitskiy, Lucas Beyer, Alexander Kolesnikov, Dirk Weissenborn, Xiaohua Zhai, Thomas Unterthiner, Mostafa Dehghani, Matthias Minderer, Georg Heigold, Sylvain Gelly, et al. An image is worth 16x16 words: Transformers for image recognition at scale. *arXiv preprint arXiv:2010.11929*, 2020. 6
- [5] Mehrdad Farajtabar, Navid Azizan, A. Mott, and Ang Li. Orthogonal gradient descent for continual learning. *Cornell University - arXiv, Cornell University - arXiv*, 2019. 3
- [6] Enrico Fini, Victor G Turrissi Da Costa, Xavier Alameda-Pineda, Elisa Ricci, Karteek Alahari, and Julien Mairal. Self-supervised models are continual learners. In *Proceedings of the IEEE/CVF Conference on Computer Vision and Pattern Recognition*, pages 9621–9630, 2022. 2
- [7] Qiankun Gao, Chen Zhao, Yifan Sun, Teng Xi, Gang Zhang, Bernard Ghanem, and Jian Zhang. A unified continual learning framework with general parameter-efficient tuning. In *Proceedings of the IEEE/CVF International Conference on Computer Vision*, pages 11483–11493, 2023. 6, 7, 8
- [8] Jiangpeng He. Gradient reweighting: Towards imbalanced class-incremental learning. In *Proceedings of the IEEE/CVF Conference on Computer Vision and Pattern Recognition*, pages 16668–16677, 2024. 1, 2, 3, 6, 7, 8
- [9] Kaiming He, Haoqi Fan, Yuxin Wu, Saining Xie, and Ross Girshick. Momentum contrast for unsupervised visual representation learning. In *Proceedings of the IEEE/CVF conference on computer vision and pattern recognition*, pages 9729–9738, 2020. 6
- [10] Kaiming He, Xinlei Chen, Saining Xie, Yanghao Li, Piotr Dollár, and Ross Girshick. Masked autoencoders are scalable vision learners. In *Proceedings of the IEEE/CVF conference on computer vision and pattern recognition*, pages 16000–16009, 2022. 6
- [11] Menglin Jia, Luming Tang, Bor-Chun Chen, Claire Cardie, Serge Belongie, Bharath Hariharan, and Ser-Nam Lim. Visual prompt tuning. In *European Conference on Computer Vision (ECCV)*, 2022. 3
- [12] Suguru Kanoga, Ryo Karakida, Takayuki Hoshino, Yuto Okawa, and Mitsunori Tada. Deep generative replay-based class-incremental continual learning in semg-based pattern recognition. In *2024 46th Annual International Conference of the IEEE Engineering in Medicine and Biology Society (EMBC)*, pages 1–4, 2024. 2
- [13] Ronald Kemker and Christopher Kanan. Fearnert: Brain-inspired model for incremental learning. *International Conference on Learning Representations, International Conference on Learning Representations*, 2017. 2
- [14] Diederik P. Kingma and Jimmy Ba. Adam: A method for stochastic optimization. *arXiv: Learning, arXiv: Learning*, 2014. 2, 6
- [15] James Kirkpatrick, Razvan Pascanu, Neil Rabinowitz, Joel Veness, Guillaume Desjardins, Andrei A Rusu, Kieran Milan, John Quan, Tiago Ramalho, Agnieszka Grabska-Barwinska, et al. Overcoming catastrophic forgetting in neural networks. *Proceedings of the national academy of sciences*, 114(13):3521–3526, 2017. 1, 3
- [16] Yann LeCun, Yoshua Bengio, and Geoffrey Hinton. Deep learning. *Nature*, page 436–444, 2015. 2, 6
- [17] Brian Lester, Rami Al-Rfou, and Noah Constant. The power of scale for parameter-efficient prompt tuning. In *Proceedings of the 2021 Conference on Empirical Methods in Natural Language Processing*, 2021. 3
- [18] Bo Liu, Xingchao Liu, Xiaojie Jin, Peter Stone, and Qiang Liu. Conflict-averse gradient descent for multi-task learning. *Advances in Neural Information Processing Systems*, 34, 2021. 5
- [19] Vincenzo Lomonaco and Davide Maltoni. Core50: a new dataset and benchmark for continuous object recognition. In *Conference on robot learning*, pages 17–26. PMLR, 2017. 6, 8
- [20] David Lopez-Paz and Marc’Aurelio Ranzato. Gradient episodic memory for continual learning. In *NIPS*, 2017. 3
- [21] David Lopez-Paz and Marc’Aurelio Ranzato. Gradient episodic memory for continual learning. *Neural Information Processing Systems, Neural Information Processing Systems*, 2017. 2
- [22] Sheng Luo, Wei Chen, Wanxin Tian, Rui Liu, Luanxuan Hou, Xiubao Zhang, Haifeng Shen, Ruiqi Wu, Shuyi Geng,

- Yi Zhou, Ling Shao, Yi Yang, Bojun Gao, Qun Li, and Guobin Wu. Delving into multi-modal multi-task foundation models for road scene understanding: From learning paradigm perspectives. *IEEE Transactions on Intelligent Vehicles*, pages 1–25, 2024. 2
- [23] Imad Eddine Marouf, Subhankar Roy, Enzo Tartaglione, and Stéphane Lathuilière. Weighted ensemble models are strong continual learners. In *European Conference on Computer Vision*, pages 306–324. Springer, 2024. 6
- [24] M Jehanzeb Mirza, Marc Masana, Horst Possegger, and Horst Bischof. An efficient domain-incremental learning approach to drive in all weather conditions. In *Proceedings of the IEEE/CVF conference on computer vision and pattern recognition*, pages 3001–3011, 2022. 2
- [25] Shuaicheng Niu, Jiaxiang Wu, Yifan Zhang, Zhiqian Wen, Yaofo Chen, Peilin Zhao, and Mingkui Tan. Towards stable test-time adaptation in dynamic wild world. In *International Conference on Learning Representations*, 2023. 2, 5
- [26] Min-Yeong Park, Jae-Ho Lee, and Gyeong-Moon Park. Versatile incremental learning: Towards class and domain-agnostic incremental learning. In *European Conference on Computer Vision*, pages 271–288. Springer, 2024. 2, 3, 6, 7, 8
- [27] Xingchao Peng, Qinxun Bai, Xide Xia, Zijun Huang, Kate Saenko, and Bo Wang. Moment matching for multi-source domain adaptation. In *Proceedings of the IEEE/CVF international conference on computer vision*, pages 1406–1415, 2019. 4, 6, 8
- [28] Alec Radford, Jong Wook Kim, Chris Hallacy, Aditya Ramesh, Gabriel Goh, Sandhini Agarwal, Girish Sastry, Amanda Askell, Pamela Mishkin, Jack Clark, et al. Learning transferable visual models from natural language supervision. In *International conference on machine learning*, pages 8748–8763. PmLR, 2021. 6
- [29] Sylvestre-Alvise Rebuffi, Alexander Kolesnikov, Georg Sperl, and Christoph H Lampert. icarl: Incremental classifier and representation learning. In *Proceedings of the IEEE conference on Computer Vision and Pattern Recognition*, pages 2001–2010, 2017. 1
- [30] Subhankar Roy, Aliaksandr Siarohin, Enver Sangineto, Samuel Rota Bulò, Nicu Sebe, and Elisa Ricci. Unsupervised domain adaptation using feature-whitening and consensus loss. *Cornell University - arXiv, Cornell University - arXiv*, 2019. 3
- [31] Subhankar Roy, Martin Trapp, Andrea Pilzer, Juho Kannala, Nicu Sebe, Elisa Ricci, and Arno Solin. Uncertainty-guided source-free domain adaptation. 2022. 3
- [32] Gobinda Saha, Isha Garg, and Kaushik Roy. Gradient projection memory for continual learning. *Cornell University - arXiv, Cornell University - arXiv*, 2021. 3
- [33] James Seale Smith, Leonid Karlinsky, Vyshnavi Gutta, Paola Cascante-Bonilla, Donghyun Kim, Assaf Arbelle, Rameswar Panda, Rogerio Feris, and Zsolt Kira. Coda-prompt: Continual decomposed attention-based prompting for rehearsal-free continual learning. In *Proceedings of the IEEE/CVF Conference on Computer Vision and Pattern Recognition*, pages 11909–11919, 2023. 1, 2, 3, 6, 7, 8
- [34] Riccardo Volpi, Diane Larlus, and Grégory Rogez. Continual adaptation of visual representations via domain randomization and meta-learning. In *Proceedings of the IEEE/CVF Conference on Computer Vision and Pattern Recognition*, pages 4443–4453, 2021. 6, 8
- [35] Dequan Wang, Evan Shelhamer, Shaoteng Liu, Bruno Olshausen, and Trevor Darrell. Tent: Fully test-time adaptation by entropy minimization. In *International Conference on Learning Representations*, 2021. 2, 3, 5
- [36] Liyuan Wang, Xingxing Zhang, Hang Su, and Jun Zhu. A comprehensive survey of continual learning: Theory, method and application. *IEEE Transactions on Pattern Analysis and Machine Intelligence*, 46(8):5362–5383, 2024. 3
- [37] Yabin Wang, Zhiwu Huang, and Xiaopeng Hong. S-prompts learning with pre-trained transformers: An occam’s razor for domain incremental learning. *Advances in Neural Information Processing Systems*, 35:5682–5695, 2022. 1, 2, 6
- [38] Zifeng Wang, Zizhao Zhang, Sayna Ebrahimi, Ruoxi Sun, Han Zhang, Chen-Yu Lee, Xiaoqi Ren, Guolong Su, Vincent Perot, Jennifer Dy, et al. Dualprompt: Complementary prompting for rehearsal-free continual learning. In *European Conference on Computer Vision*, pages 631–648. Springer, 2022. 1, 2, 3, 6, 7, 8
- [39] Zifeng Wang, Zizhao Zhang, Chen-Yu Lee, Han Zhang, Ruoxi Sun, Xiaoqi Ren, Guolong Su, Vincent Perot, Jennifer Dy, and Tomas Pfister. Learning to prompt for continual learning. In *Proceedings of the IEEE/CVF conference on computer vision and pattern recognition*, pages 139–149, 2022. 2, 3, 6, 7, 8
- [40] Shipeng Yan, Jiangwei Xie, and Xuming He. Der: Dynamically expandable representation for class incremental learning. 2021. 1
- [41] Enneng Yang, Zhenyi Wang, Li Shen, Shiwei Liu, Guibing Guo, Xingwei Wang, and Dacheng Tao. Adamerging: Adaptive model merging for multi-task learning. *The Twelfth International Conference on Learning Representations*, 2024. 3
- [42] Zangwei Zheng, Mingyuan Ma, Kai Wang, Ziheng Qin, Xiangyu Yue, and Yang You. Preventing zero-shot transfer degradation in continual learning of vision-language models. *arXiv preprint arXiv:2303.06628*, 2023. 3
- [43] Kaiyang Zhou, Jingkang Yang, Chen Change Loy, and Ziwei Liu. Learning to prompt for vision-language models. *International Journal of Computer Vision*, page 2337–2348, 2022. 3